Initial Design and Quick Analysis of SAW Ultra–Wideband HFM Transducers

Arturas JANELIAUSKAS, Vytautas MARKEVICIUS, Dangirutis NAVIKAS, Darius ANDRIUKAITIS, Algimantas VALINEVICIUS, Mindaugas ZILYS

Dept. of Electronics Engineering, Kaunas University of Technology, Studentų Street 50-438, LT-51368 Kaunas, Lithuania

arturas.janeliauskas@ktu.lt, vytautas.markevicius@ktu.lt, dangirutis.navikas@ktu.lt, darius.andriukaitis@ktu.lt, algimantas.valinevicius@ktu.lt, mindaugas.zilys@ktu.lt

Submitted December 17, 2016 / Accepted May 18, 2017

Abstract. *This paper presents techniques for initial design and quick fundamental and harmonic operation analysis of surface acoustic waves ultra-wideband hyperbolically frequency modulated (HFM) interdigital transducer (IDT). The primary analysis is based on the quasi–static method. Quasi–electrostatic charge's density distribution was approximated by Chebyshev polynomials and the method of Green's function. It assesses the non uniform charge distribution of electrodes, electric field interaction and the end effects of a whole transducer. It was found that numerical integration (e.g. Romberg, Gauss–Chebyshev) requires a lot of machine time for calculation of the Chebyshev polynomial and the Green's function convolution when integration includes coordinates of a large number of neighboring electrodes. In order to accelerate the charge density calculation, the analytic expressions are derived. Evaluation of HFM transducer fundamental and harmonics' operation amplitude response with simulation single–dispersive interdigital chirp filter structure is presented. Elapsed time of 2000 frequency response point simulations of HFM IDT with 589 electrodes is only 54 seconds (0.027 s/point) on PC with CPU Intel Core I7–4770S. Amplitude response is compared with linear frequency modulated (LFM) IDT response. It was determined that the HFM transducer characteristic is less distorted in comparison with LFM transducer.*

Keywords

Surface acoustic wave (SAW), hyperbolically frequency modulated waveforms (HFM), interdigital transducer (IDT), quasi-static method, Chebyshev polynomial approximation, Green's function, interdigital chirp filter, harmonics' operation

1. Introduction

New emerging applications of the Surface Acoustic Waves (SAW) technology include SAW filters, sensors and tag systems that use Ultra-Wideband (UWB) frequency spectrum for communication. UWB technology improves resistance to interference, performance in noisy environments and reading distances without increasing transmitter power [1], [2]. Acceptable processing gain B×T for UWB technology tags system is 50–200. For such devices Hyperbolically Frequency Modulated (HFM) interdigital transducers (IDT's) have significant advantages: they are practically insensitive to temperature variations, which expand or compress signals in time and are ideal for SAW sensor and SAW tag industrial application, where the temperature varies over a large range [3].

As shown below, HFM IDT can include hundreds or even thousands nonperiodic electrodes. Design process of such transducers requires efficient simulation models. Today, there is only one theoretical model that allows analysis of such transducers. It is known as FEM (Finite–Element Method) and BEM (Boundary Element Method) [4]. Researchers are looking for ways to speed up the FEM/BEM analysis of nonperiodic SAW structures [5], but accurate analysis of long dispersive transducers is still time-consuming [6]. Moreover, the design process requires a trial and error method to find the results. In fact, simulation is too slow to use in practical design of UWB SAW devices. It requires a lot of time to check design changes and complicates the optimization process of the devices. Therefore, for the initial evaluation it is required to have a fast simplified model as a supporting tool (like delta-function model for equidistant weighted design of transducers). To achieve shorter calculation time and get a primary frequency response quasi-static analysis can be used [7]. Key conditions for which the method gives reliable results follow from quasi-static analysis prerequisites that the elastic body is quasi isotropic, the vector of SAW energy flow coincides with the vector of wave propagation direction, elastic medium is quasi linear and the coefficient of electromechanical coupling is poor. In this case it was proved [7] that the frequency response depends only on the charge distribution on the electrodes. Therefore, while creating the transducer model it is possible to consider the acoustic wave not connected with electrical field. Then the problem is divided into the problems of electrostatics and acoustic wave excitation. In ours case, the SAW field is not

of interest; only advance electrical properties are required. According to this simplified method, Fourier transforms (FT) of charge distribution mainly describe the most important characteristic in applications – the frequency response. This method is well suited for weak piezoelectric and is useful for quick initial design of the SAW devices. However, there is no general analytic procedure for calculation of the IDT characteristics which is suitable for arbitrary nonperiodic electrode structures, so solving the integral equations with the electrical and mechanical boundary conditions is achieved using numerical methods. Using Chebyshev interpolation of the charge distribution, the concept of semi-infinite Green's function, and the finite element method for taking into account the mechanical perturbation of electrodes, rigorous numerical model for 2D finite transducers analysis, including precise charge distribution simulation on electrodes of finite structures up to 200 electrodes has been presented in [8]. As mentioned in [8], in order to limit the CPU time, the development of powerful methods to integrate the semi-infinite Green's function is the most relevant. As shown in this work, the same applies to the simplified methods that use only electrostatic Green's function contribution.

Table 1 shows that large computation of charge density distribution is the common problem of dispersive IDTs' analysis. Moreover, the method is appropriate only when quick and accurate FT exists.

For a quick analysis of long dispersive IDTs, we have improved the method proposed by W. R. Smith and W. F. Pedler in 1975 [12]. The method was developed primarily for analysis of non-dispersive IDTs with arbitrary metallization ratios and polarity sequences in the environment of a few electrodes. We found that some of the integrals converge slowly and are the main contribution to time-consuming calculations. Therefore, we found the analytical expressions of them, allowing greatly accelerated calculations, increased accuracy and stability of this method and allowing fast analysis of long dispersive transducers. The method is very simplified; a lot of effects are neglected. Real insertion loss is not taken into account and operates only with relative value of losses. To obtain optimum performance of characteristics of the device in the first approach, the necessary corrections will be applied via digital signal processing methods. The method is fast and useful to facilitate the synthesis of dispersive transducers an acceptable processing gain $BT = 50–100$ for UWB technology system. The limit of the electrode numbers depends on the computational algorithms, software package, operating system and computer resources. The calculations were performed using Mathcad package and its operator "lsolve", which returns the solution for the linear system of equations, using LU decomposition. In this case a system of linear equations can be solved without difficulty if the number of equations and variables does not exceed 4080 (maximum number of electrodes $N = 680$ with 6 points each) due to 2 GB memory limit of .NET 1.0 objects. Now PTC Mathcad Prime 3.1 enables large data handling beyond this 2 GB limit. These new possibilities could be investigated in the future.

Approach	Approach specification		
	Technique	**Quick and accurate FT exists?**	**Suitability for dispersive IDT's**
Direct evaluation of the charge spatial spectrum based on the infinite periodic system of strip groups approaches [9], [10]	The solution is constructed in a spectral domain as linear combinations of template functions, whose summation coefficients satisfy boundary conditions in a spatial domain	Solution is in the spectral domain, but quick and accurate inverse FT to the spatial domain is necessary	Yes, but the infinite periodic system of a strip groups' approach has a limited number of independent electrodes. Requires large computation
Keldysh and Sedov solution of the mixed boundary problem of the analytic function theory [8]	Exact analytic solution of an electrostatic problem with a finite number of electrodes in a spatial domain	Only on single electrodes	Yes, but exact analytic solution requires large computation
Bausk-Kolosovsky-Kozlov-Solie algorithm [11]	Keldysh and Sedov solution, the Gauss integration method, the expansion of functions into a series of Chebyshev polynomials	Yes	Yes, but the algorithm conserves stability if the number of electrodes is less than 51 only. Requires large computation
Electrostatic Green's function and Chebyshev polynomials approximation [12]	Approximation using Chebyshev polynomials, electrostatic Green's function and boundary conditions in spatial domain	Yes	Method was used for environment of few electrodes only

Tab. 1. Basic simplified approaches to evaluation of the spatial spectrum of IDT's charge density distribution.

In this paper, a simplified method of the calculation of the response of HFM delay line is presented. The method allows evaluating of relative insertion loss only. The limit of the electrode numbers is 680.

2. Initial Design and Analysis of SAW Ultra-Wideband HFM Transducers

2.1 Design of HFM Transducers

The key step in design of a fundamental frequency dispersive transducer is the determination of the electrode

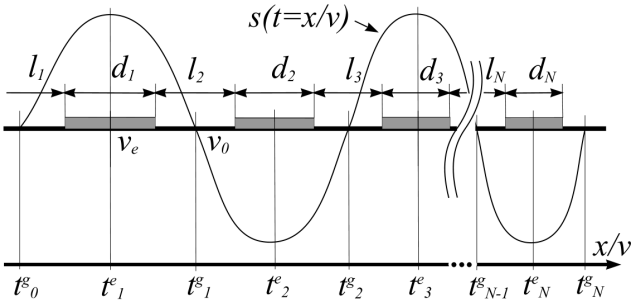

Fig. 1. The electrode and gap center positions of the single electrode transducer case.

positions. If the transducer operates in harmonics, the uniformity of a metallization ratio has a great impact. If IDT is properly designed, this ratio must remain constant with changes of the electrode step. Otherwise, the element factor per IDT period will vary and transducer's amplitude response at harmonic's operation will be distorted. Consequently, for such IDTs both the electrode and gap centers' positions must be determined and only then electrode's width with a fixed metallization ratio can be calculated. In the first approximation, the electrode and the positions of gap centers are determined from the required impulse response $s(t)$ which corresponds to ideal theoretical HFM waveforms such as [13], where the signal acquires pure real and imaginary values (signal phase is $k\pi$ and $k\pi+\pi/2$, k is an integer) (Fig. 1).

The time samples which determine the n-th electrode t^{e}_n and gap t^{g}_n center positions within the time domain can be found:

$$t^{\mathrm{e}}_n = \frac{\exp\left(\frac{nb}{2}\right)-1}{b\left(f_0+B/2\right)}, \tag{1}$$

$$t^{\mathrm{g}}_n = \frac{\exp\left(\frac{(n+1/2)b}{2}\right)-1}{b\left(f_0+B/2\right)}, \tag{2}$$

$$b = \frac{f_1-f_2}{f_1 f_2 T} = B\left[T\left(f_0^2-\frac{B^2}{4}\right)\right]^{-1} \tag{3}$$

where f_1, f_2 is the start and end frequency of the HFM waveform, respectively; $B=f_1-f_2$ denotes the used frequency band of the chirp signal, T is its duration and f_0 is the center frequency.

The electrode and gap width d_n, l_n for a single electrode transducer case (Fig. 1) are determined as:

$$d_n = v_{\mathrm{e}}\left(t^{\mathrm{g}}_n - t^{\mathrm{g}}_{n-1}\right)\eta, \tag{4}$$

$$l_n = v_0\left(t^{\mathrm{e}}_n - t^{\mathrm{e}}_{n-1}\right)(1-\eta) \tag{5}$$

where v_{e}, v_0 are the SAW velocity of the metallized and free surface respectively, $\eta = d_n/(d_n+l_n)$ is the metallization ratio (the same for all electrodes).

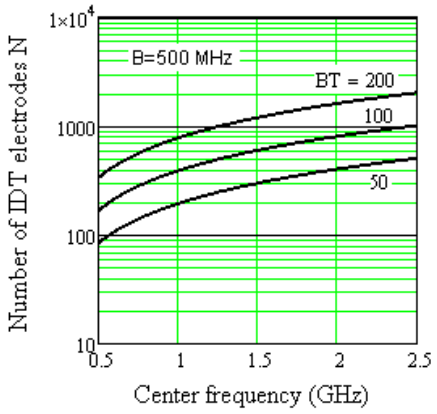

Fig. 2. The HFM IDT electrode number at an acceptable processing gain for UWB technology tags system.

Number of IDT electrodes N is determined by the pulse duration. When $t^{\mathrm{e}}_N - t^{\mathrm{e}}_1 = T$ and $t^{\mathrm{e}}_1 = 0$, by (1) N is obtained

$$N = \left\lceil \left| -2\frac{T}{B}\left(f_0^2-\frac{B^2}{4}\right)\ln\left(1-\frac{B}{f_0+\frac{B}{2}}\right)\right| \right\rceil. \tag{6}$$

The HFM IDT electrode number at an acceptable processing gain BT for UWB technology tags system determined by (6) is shown in Fig. 2.

2.2 Fundamental and Harmonic Operation Analysis of HFM Transducers

The primary analysis is based on the quasi-static method [7]. Second-order effects are ignored. In the approximation considered here, the electric charge distribution does not depend on ω and is determined only by the geometry of the electrodes. The electrodes are assumed to be parallel, perfectly conductive, massless, and situated on the surface of a dielectric halfspace. In this case, the single transducer (Fig. 3) frequency response is given by

$$H(\mathrm{j}\omega) = (\omega W \Gamma_s)^{\frac{1}{2}} \sum_{n=1}^{N} \sigma_n(\omega)\exp\left(-\mathrm{j}\frac{\omega}{v}c_n\right) \tag{7}$$

where Γ_s is a constant depending on the material, W is transducer electrodes' overlap, ω is frequency, $\sigma_n(\omega)$ is Fourier's transform of electric charge density distribution on the n-th electrode, v is SAW effective velocity, c_n are the n-th electrode positions (coordinate of the electrode's center).

The form of the function $\sigma_n(\omega,\eta)$ is fundamental to the operation of all types of IDTs, so charge density distribution must be counted as accurately as possible.

The potential and charge density relation of the transducer electrodes (Fig. 3) is written under the form of a Fredholm homogeneous integral equation with function $\ln|x-x'|$ as the kernel

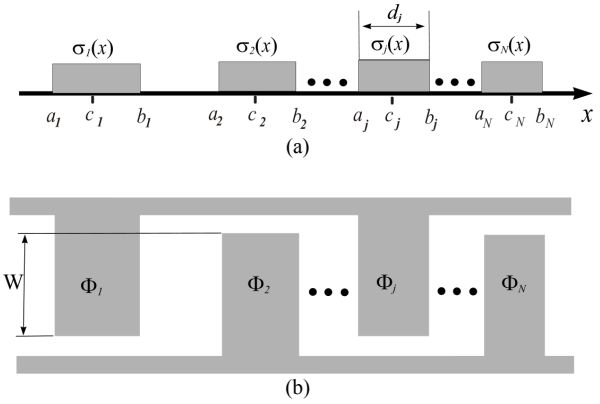

Fig. 3. Dispersive interdigital transducer with single-electrode type: a) cut view; b) upper view.

$$\Phi_i(x) = -\frac{1}{\pi\left(\varepsilon_0 + \varepsilon_{\mathrm{p}}^{\mathrm{T}}\right)} \sum_{j=1}^{N} \int_{a_j}^{b_j} \sigma_j(x') \ln\left|x - x'\right| \mathrm{d}x' \quad (8)$$

where $\Phi_i(x)$ is the i-th electrode's potential when $a_i < x < b_i$ and $i = 1,2,\ldots,N$, $\sigma_j(x')$ is the j-th electrode's charge density distribution, $\varepsilon_{\mathrm{p}}^{\mathrm{T}}$ is dielectric permittivity at constant mechanical tension. Coordinates x', x must be normalized vs the j-th electrode's width d_j and center c_j ($j = 1,2,\ldots, N$) to introduce dimensionless variables [12].

The divergence of charge density distribution at the electrode edges complicates the solution of (8). Conventional numerical methods of this case converge slowly and dramatically increase duration of calculations. Charge density Chebyshev polynomials' approximation with square root weight function in a denominator is more effective. High accuracy is achieved even when using a fifth order polynomial [12].

Using Chebyshev polynomials on the basis of the quasi-electrostatic field description presented in [12], the charge density on the j-th electrode is expressed as

$$\sigma_j(x') = 2\pi \frac{\left(\varepsilon_0 + \varepsilon_{\mathrm{p}}^{\mathrm{T}}\right)}{d_j \sqrt{1-(x')^2}} \sum_{m=0}^{5} \alpha_m^{(j)} \mathrm{T}_m(x') \quad (9)$$

where $\mathrm{T}_m(x')$ is the m-th order Chebyshev polynomial, x' is the normalized coordinate ($-1 < x' < 1$), $\alpha_m^{(j)}$ is the j-th electrode's polynomial coefficients.

Coefficients $\alpha_m^{(j)}$ are calculated by solving the equation systems with different electrode potentials and the additional condition – sum of charges of all electrodes must equal zero [12]. In order to obtain solutions, it is necessary to calculate the integrals, which general forms

$$y_m(x) = \int_{-1}^{1} \frac{\mathrm{T}_m(x')}{\sqrt{1-(x')^2}} \ln\left|x - x'\right| \mathrm{d}x', \; m = 0, 1, 2, \ldots, 5. \quad (10)$$

When $|x| < 1$ coordinates x and x' are on the same electrodes. In this case, integrals (10) are tabulated and may be evaluated in a closed form

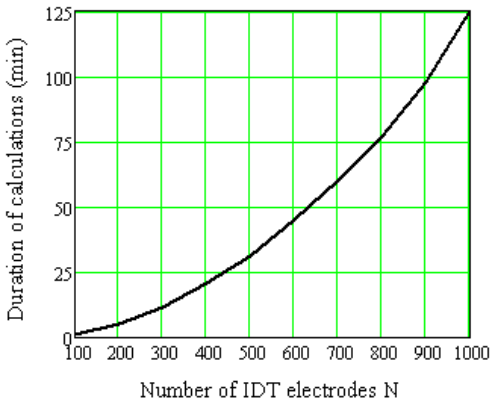

Fig. 4. The duration of numerical integration using Mathcad internal Romberg's integration algorithm.

$$\frac{1}{\pi} \int_{-1}^{1} \frac{\mathrm{T}_m(x')}{\sqrt{1-(x')^2}} \ln\left|x - x'\right| \mathrm{d}x' = \begin{cases} -\ln 2, & m = 0, \\ -\dfrac{1}{m} \mathrm{T}_m(x), & m \neq 0. \end{cases} \quad (11)$$

When $|x| > 1$ the kernel of integrals (10) includes coordinates x of neighboring electrodes against the electrode with coordinate x'. In this case analytical expressions of (10) were unknown and only numerical integrations were possible. We found that due to the charge distribution singularities on electrodes' edges whose form is given by the denominator $\sqrt{1-(x')^2}$, integrals (10) converge slowly and have the main contribution to time-consuming calculations (especially for a large electrode number). Our assessment of the numerical integration (10) using Mathcad internal Romberg's integration algorithm is presented in Fig. 4.

Similar behaviors were obtained using Gauss-Chebyshev quadrature formula for numerical integration. Calculations were performed with Mathcad installed on Windows PC (Motherboard Ga–Z87–HD3, CPU Intel Core I7–4770S 3.1 GHz, 4 x DDR3 25.6 GB/s).

As it can be seen from Fig. 4, duration of calculations is unacceptably long for simplified analysis and quick initial design of the dispersive transducers. Therefore, it is appropriate to rule out numerical integration methods and try to derive the analytical expressions of (10), when $|x| > 1$. Using integration by parts and the substitution method, we have obtained the following expressions, all for $|x| > 1$:

$$y_0(x) = \pi \ln \frac{|x| + \sqrt{x^2 - 1}}{2}, \quad (12)$$

$$y_1(x) = -\pi\left(x - \mathrm{sign}(x)\sqrt{x^2 - 1}\right), \quad (13)$$

$$y_2(x) = \frac{\pi}{2} - \pi\left(x^2 - |x|\sqrt{x^2 - 1}\right), \quad (14)$$

$$y_3(x) = \pi\left(-\frac{4}{3}x^3 + x + \mathrm{sign}(x)\left(\frac{4}{3}\left(\sqrt{x^2-1}\right)^3 + \sqrt{x^2-1}\right)\right), \quad (15)$$

$$y_4(x)=\pi\left(-2x^4+2x^2-\frac{1}{4}+|x|\left(\sqrt{x^2-1}\right)^3+|x|^3\sqrt{x^2-1}\right), \quad (16)$$

$$y_5(x)=\pi\left(-\frac{16}{5}x^5+4x^3-x-\operatorname{sign}(x)\left(\frac{12}{5}\left(\sqrt{x^2-1}\right)^3-\left(\frac{16}{5}x^4-\frac{11}{5}\right)\sqrt{x^2-1}\right)\right). \quad (17)$$

Using the analytical expressions (11)–(17), the integrals (10) can be evaluated in a closed form, and the integral equation (8) may be substituted by a system of algebraic equations to determine Chebyshev polynomial coefficients' $\alpha_m^{(j)}$ and electric charge density distribution (9) on the electrodes. Finally the Fourier transform of (9) and coefficients' $\alpha_m^{(j)}$ allows quick and easy calculation of $\sigma_j(\omega)$ to determine the frequency response by (7):

$$\sigma_j(\omega)=\pi^2(\varepsilon_0+\varepsilon_p^{\mathrm{T}})\sum_{m=0}^{5}\left(-\sqrt{-1}\right)^m\alpha_m^{(j)}J_m\left(\frac{\omega}{2v}d_j\right) \quad (18)$$

where $J_m\left(\frac{\omega}{2v}d_j\right)$ is the m-th order Bessel functions of the first kind, $j=1,2,\ldots,N$.

Formula (18) and above presents the calculation methodology of polynomial coefficients', greatly accelerates the calculations of transducer frequency response and increases stability of the method.

2.3 Approximation Error Analysis

Total approximation error (error in the method and calculations) can be evaluated in comparison with the exact solution – an ideal model. It can be found only for the simplest topologies, for example consisting of a few strips [10] or for an infinite periodic system of electrodes [7]. Approximated solution comparison with exact solution of infinite periodic system is more adequate, because a large number of simulated electrodes have more influence on computational errors, which may occur in this case.

Suppose that the active electrode with potential $\Phi_{en}=+1$ V is located on the center of the infinite array of regular electrodes (Fig. 5). On both sides of the central electrode, the array of passive electrodes with potential $\Phi_{en\pm j}=0$ V, $j=1,2,\ldots$ is arranged. Out of charge distribution analysis using (8) shows that the normalized charge density under a given electrode depends only on the dimensions and potential of that electrode and its nearest and next-nearest neighbors (Fig. 5).

In the present case, increasing distance from the center electrode on both sides, the charge density of neighboring electrodes decreases rapidly: local electric fields are almost uninfluenced by the electrodes more distant than the next-nearest neighbors. Therefore, the total approximation error can be found by calculating the difference between the solutions for finite and infinite periodic systems.

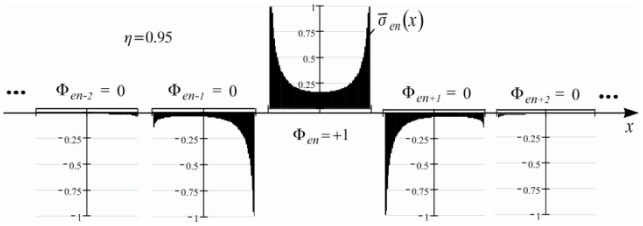

Fig. 5. The array of regular electrodes and electric charge density distribution.

Because the forms of the functions $\sigma_j(\omega)$ determine the frequency response of the transducer, to estimate an approximation error, normalized Fourier's transform of electric charge density distribution (hereinafter referred to as element factor) on the central electrode for finite $\tilde{\sigma}_{en}(\omega,\eta)$ (the approximated solution based on (18)) can be compared to infinite $\bar{\sigma}_{en}(\omega,\eta)$ (the exact solution presented in [7]) periodic systems of electrodes.

Then the absolute error $\varepsilon(\omega_M,\eta)$ of the element factor can be expressed as

$$\varepsilon(\omega_M,\eta)=\left|\bar{\sigma}_{en}(\omega,\eta)-\tilde{\sigma}_{en}(\omega,\eta)\right| =\left|\left[\frac{\pi P_m(\cos\pi\eta)}{K\left(\sqrt{(1+\cos\pi\eta)/2}\right)}-\pi^2\sum_{n=0}^{2}(-1)^n\alpha_{2n}J_{2n}\left(\frac{1}{2}M\pi\eta\right)\right]\right| \quad (19)$$

where $P_m(\cos(\pi\eta))$ is Legendre polynomial, $m=(M-1)/2$, $M=1,3,5,\ldots$ is harmonic number; $K\left(\sqrt{(1+\cos\pi\eta)/2}\right)$ is the complete elliptic integral of the first kind.

Investigations of these errors for finite periodic systems contain 600 electrodes shown in Fig. 6 and Fig. 7.

As can be seen from Fig. 7, the total absolute error does not exceed 0.04 up to metallization ratio 0.85. That is 2–3 % of $\tilde{\sigma}_{en}(\omega,\eta)$ value. Therefore, approximated solution can be considered to be very close to the theoretical if $\eta \le 0.85$.

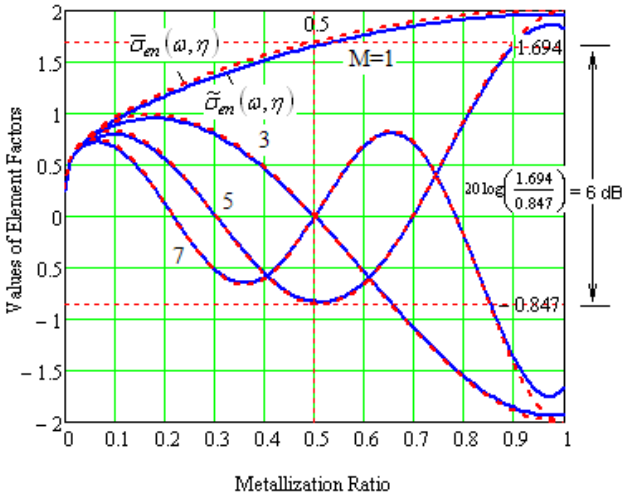

Fig. 6. The values of element factors $\bar{\sigma}_{en}(\omega,\eta)$ and $\tilde{\sigma}_{en}(\omega,\eta)$.

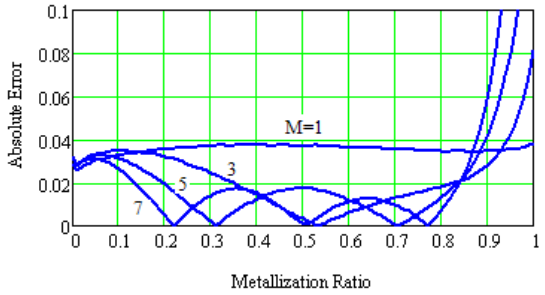

Fig. 7. The absolute error $\varepsilon(\omega_M, \eta)$ of element factor $\tilde{\sigma}_{en}(\omega,\eta)$.

3. Evaluation of HFM Transducer Characteristics

The test structure for HFM IDT characteristics' evaluation is shown in Fig. 8. It presents a single-dispersive interdigital chirp filter, having a nonapodized up-chirp HFM transducer IDT1 and a uniform wide-band transducer IDT2.

When a voltage U_1 is applied to the transducer IDT1, the current I_2 produced by transducer IDT2 is assumed to be shorted. The device response is given by the product of the transducer responses [7]

$$H_{\Sigma}(\mathrm{j}\omega) = \frac{I_2}{U_1} = H_1(\mathrm{j}\omega) H_2(\mathrm{j}\omega) \exp\left(-\mathrm{j}\frac{\omega}{v} L\right) \quad (20)$$

where $H_1(\mathrm{j}\omega)$, $H_2(\mathrm{j}\omega)$ are the responses of the transducers IDT1 and IDT2 and are defined by (7).

The test structure of the chirp filter (Fig. 8) was created and simulated in order to show the possibilities of our method only. 2000 frequency response points were simulated. Estimated old and new model characteristics are the same, the only very significant difference being the duration of calculation.

The main parameters of the model: HFM IDT1 fundamental center frequency $f_0 = 300$ MHz, bandwidth $B =$ 100 MHz, dispersion $T = 1$ μs, number of electrodes $N = 589$, metallization ratio $\eta = 0.5$. Uniform wide-band transducer IDT2 consists of three electrodes. HFM transducer IDT1 was synthesized according to the expressions presented in Sec. 2.1. At this stage it is important for obtained characteristics to be close to theoretical. The initial theoretical HFM signal spectrum and group delay with the simulated transducer IDT1 of the same characteristics was

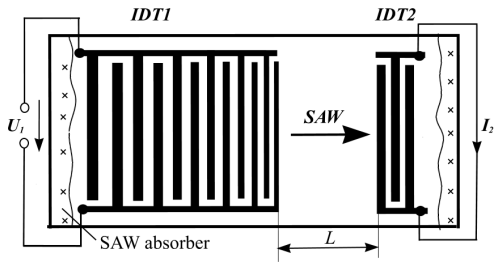

Fig. 8. Single-dispersive interdigital chirp filter test structure for transducer characteristic evaluation.

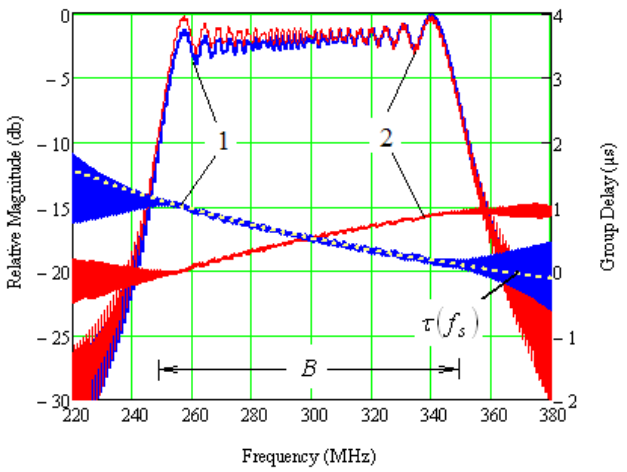

Fig. 9. Comparison of the initial HFM signal spectrum magnitude and group delay with the simulated with the same characteristics of simulated dispersive transducer IDT1: 1 – simulated frequency response $H_1(\mathrm{j}\omega)$ of transducer IDT1, 2 – theoretical HFM signal (was used for IDT1 synthesis) spectrum, $\tau(f_S)$ – instantaneous frequency delay of the ideal HFM signal for comparison.

compared in Fig. 9. This initial HFM signal with parameters $f_0 = 300$ MHz, $B = 100$ MHz, $T = 1$ μs was used for IDT1 layout design.

As it can be seen from Fig. 9 small differences only occur due to non uniformity of electric charge density distribution. Group delay of initial HFM signal is opposite.

There are two ways to prove that the simulated frequency response really corresponds to HFM signal:

1. Transform simulated frequency response into the time domain, find instantaneous frequency and periods as functions of delay time and compare it with ideal HFM signal instantaneous frequency – time dependence. In this case, accuracy in a time domain depends on the simulated frequency response band and the number of points. Frequency band should be as covering the entire passband and stopband regions with as many as possible frequency points.
2. The instantaneous frequency delay of the ideal HFM signal can be compared with the group delay of the simulated frequency response. The group delay is the time delay of the amplitude envelopes of the various frequency sinusoidal components of a signal through a device under test and can be calculated directly from passband regions of the simulated frequency response. In our case, this method is preferable.

Based on the HFM waveforms instantaneous frequency – time dependence presented in [13], the instantaneous frequency delay of the ideal HFM signal is expressed as

$$\tau(f_s) = \left(\frac{f_1}{f_s} - 1\right)\frac{1}{bf_1} \quad (21)$$

where f_S is the instantaneous frequency of the ideal HFM signal, $f_0 - \frac{|B|}{2} \le f_s \le f_0 + \frac{|B|}{2}$.

As it can be seen from Fig. 9, $\tau(f_S)$ uniquely corresponds to the group delay of the simulated frequency response of the chirp transducer IDT1 in a frequency band of the chirp signal B.

Convolution with initial theoretical HFM signal and impulse response of IDT1 (Fig. 10) shows that the chirp transducer IDT1 is matched with the initial HFM signal, calculated performance $H_1(j\omega)$ really corresponds to HFM and the layout is designed well.

Simulation results were compared with analogous linear frequency modulated (LFM) transducer (IDT1) and shown in Fig. 11. Elapsed time of 2000 frequency response points simulation is only 54 seconds (0.027 s/point), which is particularly fast compared with 42 minutes when numerical integrations are used to determine Chebyshev polynomial coefficients.

In Fig. 11 we can see that the model correctly predicted theoretically known 5 and 9 harmonics response of a single-electrode transducer. Constant metallization ratio of the electrodes' step provides a close to a rectangular amplitude response, so HFM transducers may be useful for

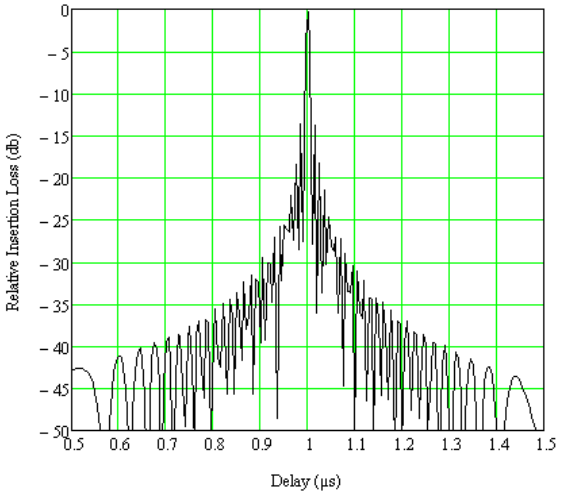

Fig. 10. Calculated convolution with the initial HFM signal and the impulse response of the chirp transducer IDT1.

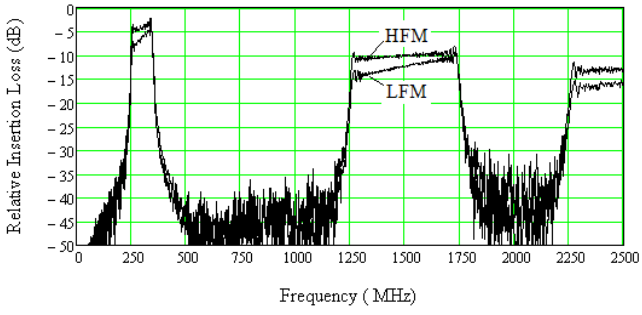

Fig. 11. Amplitude response of chirp filter with HFM and analogous LFM transducer.

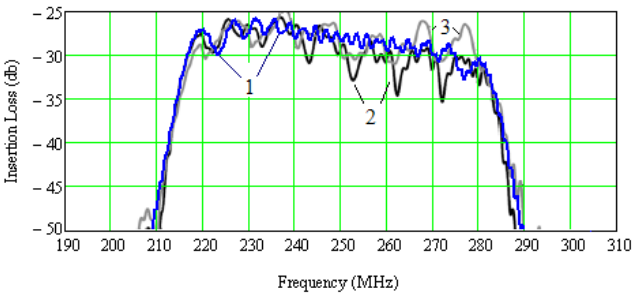

Fig. 12. The comparison of the simulated and experimentally measured frequency response [14] of the initial chirp device design utilizing quarter-wavelength aluminum electrodes on YZ $LiNbO_3$: 1 – simulated frequency response, 2 – of up-chirp (measured), 3 – of down-chirp (measured) transducers.

harmonic's operation. As shown in Fig. 6, the fifth harmonic amplitude of element factor $\tilde{\sigma}_{en}(\omega,\eta)$ is 6 dB lower than the fundamental frequency amplitude, when $\eta = 0.5$. This affects the frequency response of the transducer as well, so the insertion loss at the fifth harmonic operation increases (Fig. 11). It is also clear from Fig. 6, that operation harmonic number can be tuned by changing metallization ratio.

4. Model Validation

We carried out validation of the model using D. R. Gallagher, et al. (2008) ([14]: p. 697, Fig. 2, p. 698, Fig. 4) provided initial chirp device layout (chapters “III. Device Design Parameters and Measurement”; “IV. UWB Dispersive Transducer Design") and measurement results ([14]: p. 699, Fig. 5) (chapter “V. UWB OFC Device Design Evolution”). Only the characteristic form correlated, because our very simplified model does not give any information about the real losses. In order to compare the curves, relative insertion loss value of simulated characteristics in Fig. 12 is shifted from 0 to –25 dB.

Due to the different reflections of the electrodes and coherent bulk conversion mode of up-chirp and down-chirp transducers, experimental characteristics are slightly different [14]. Our model does not evaluate these effects, but we can see that the simulated characteristic form correlates well with the experimental data.

5. Conclusions

The main aim of creating a simplified method for initial design and quick primary analysis of dispersive transducers is achieved. The method allows fast and stable analysis of long IDTs and does not require large computing resources.

In order to achieve the aim, quasi-electrostatic charge density distribution was approximated by Chebyshev polynomials. It was found that numerical integration (e.g. Romberg, Gauss-Chebyshev) requires a lot of machine

time of the Chebyshev polynomial convolution with the Green's function calculation when integration includes coordinates of a large number of neighboring electrodes. In order to accelerate calculation, the analytical expressions are derived. The expressions have practical importance, as they allow the main characteristics of a wide range of transducer structures with a large number of electrodes to be quickly simulated.

In order to demonstrate the possibilities of the method, the amplitude response of the chirp filter was simulated and presented. It was determined that the fixed metallization ratio with changes of the electrode step provides a close to a rectangular HFM transducer's amplitude response at harmonics. Amplitude response of an HFM IDT is less distorted compared with linear frequency modulated IDT response.

The results obtained can be used for improving an equivalent circuit model to include charge density distribution and second effects for quick analysis. Analytical expressions can come in handy in further calculations.

References

[1] YAMANOUCHI, K. Low loss and wide band filters using new dispersive interdigital transducers with floating electrodes. In *Proceedings of the IEEE Ultrasonics Symposium (IUS)*. Taipei (Taiwan), 2015, p. 1–4. DOI: 10.1109/ULTSYM.2015.0358

[2] PLESSKY, V., LAMOTHE, M. Ultra-wide-band SAW RFID/sensors. In *Proceedings of the European Frequency and Time Forum (EFTF)*. Neuchatel (Switzerland), 2014, p. 16–23. DOI: 10.1109/EFTF.2014.7331416

[3] PLESSKY, V., LAMOTHE, M. Hyperbolically frequency modulated transducer in SAW sensors and tags. *Electronics Letters,* 2013, vol. 49, no. 24, p. 1503–1504. DOI: 10.1049/el.2013.2815

[4] VENTURA, P., HODE, J. M., SOLAL, M., DESBOIS, J., RIBBE, J. Numerical method for SAW propagation characterization. In *Proceedings of the IEEE Ultrasonics Symposium (IUS)*. Sendai (Japan), 1998, p. 175–186. DOI: 10.1109/ULTSYM.1998.762125

[5] KE YABING, LI HONGLANG, HE SHITANG. Fast FEM/BEM simulation of non-periodic SAW structures. In *Proceedings of the Ultrasonics Symposium (IUS)*. Dresden (Germany), 2012, p. 815 to 818. DOI: 10.1109/ULTSYM.2012.0203

[6] HARMA, S., PLESSKY, V., LI, X., HARTOGH, P. Feasibility of ultra-wideband SAW RFID tags meeting FCC rules. *IEEE Transactions on Ultrasonics, Ferroelectrics and Frequency Control,* 2009, vol. 56, no. 4, p. 812–820. DOI: 10.1109/TUFFC.2009.1104

[7] MORGAN, D. *Surface Acoustic Wave Filters with Applications to Electronic Communications and Signal Processing.* Academic Press, UK, 2007, p. 448. ISBN: 978-0-12-372537-0

[8] VENTURA, P., HODE, J. M., LOPES, B. Rigorous analysis of finite SAW devices with arbitrary electrode geometries. In *Proceedings of the IEEE Ultrasonics Symposium (IUS)*. Seattle (WA, USA), 1995, p. 257–262. DOI: 10.1109/ULTSYM.1995.495578

[9] DANICKI, E. J. Electrostatics of interdigital transducers. *IEEE Transactions on Microwave Theory and Techniques,* 2004, vol. 51, no. 4, p. 444–452. DOI: 10.1109/TUFFC.2004.1295430

[10] BIRYUKOV, S. V., POLEVOI, V. G. The electrostatic problem for the SAW interdigital transducers in an external electric field. I. A general solution for a limited number of electrodes. *IEEE Transactions on Ultrasonics, Ferroelectrics and Frequency Control,* 1996, vol. 43, no. 6, p. 1150–1159. DOI: 10.1109/58.542059

[11] BAUSK, E., KOLOSOVSKY, E., KOZLOV, A., SOLIE, L. Optimization of broadband uniform beam profile interdigital transducers weighted by assignment of electrode polarities. *IEEE Transactions on Ultrasonics, Ferroelectrics and Frequency Control,* 2002, vol. 49, p. 1–10. DOI: 10.1109/58.981378

[12] SMITH, W. R., PEDLER, W. F. Fundamental and harmonic-frequency circuit-model analysis of interdigital transducers with arbitrary metallization ratios and polarity sequences. *IEEE Transactions on Microwave Theory and Techniques,* 1975, vol. MTT-23, no. 11, p. 853–864. DOI: 10.1109/TMTT.1975.1128703

[13] XIUFENG SONG, WILLETT, P., SHENGLI ZHOU. Range bias modeling for hyperbolic frequency modulated waveforms in target tracking. In *Proceedings of the Sensor Array and Multichannel Signal Processing Workshop (SAM)*. Hoboken (NJ, USA), 2012, p. 249–252. DOI: 10.1109/SAM.2012.6250480

[14] GALLAGHER, D. R., MALOCHA, D. C., PUCCIO, D., SALDANHA, N. Orthogonal frequency coded filters for use in ultra-wideband communication systems. *IEEE Transactions on Ultrasonics, Ferroelectrics and Frequency Control*, 2008, vol. 55. no. 3, p. 696–703. DOI: 10.1109/TUFFC.2008.694

About the Authors …

Arturas JANELIAUSKAS graduated MSc in 1984 and received his PhD in Electronics Engineering in 1995. He works at the Department of Electronics Engineering, Faculty of Electrical and Electronics Engineering, Kaunas University of Technology. His research focuses on finding solutions for the issues related to the interactive electronic systems, smart environment and information technology.

Vytautas MARKEVICIUS graduated MSc in 1973 and received his PhD in Electronics Engineering in 1983. He works at the Department of Electronics Engineering, Faculty of Electrical and Electronics Engineering, Kaunas University of Technology. He is the leader of the research group on Interactive Electronic Systems. His research focuses on finding solutions for the issues related to the interactive electronic systems, integrated information systems, energy harvesting, low power management, WSN.

Dangirutis NAVIKAS graduated MSc in 1994 and received his PhD in Electronics Engineering in 1999. He works at the Department of Electronics Engineering, Faculty of Electrical and Electronics Engineering, Kaunas University of Technology. In addition, he is a head of the Department of Electronics Engineering. His research focuses on finding solutions for the issues related to the interactive design of microprocessor systems, integrated information systems or WSN.

Darius ANDRIUKAITIS graduated MSc in 2005 and received his PhD in Electronics Engineering in 2009. He works at the Department of Electronics Engineering, Faculty of Electrical and Electronics Engineering, Kaunas University of Technology. Also, he is a vice dean for research of the Faculty of Electrical and Electronics Engineering. His research focuses on finding solutions for the

issues related to the interactive electronic systems, integrated information systems or WSN.

Algimantas VALINEVICIUS graduated MSc in 1979 and received his PhD in Electronics Engineering in 1986. He works at the Department of Electronics Engineering, Faculty of Electrical and Electronics Engineering, Kaunas University of Technology. In addition, he is a dean of the Faculty of Electrical and Electronics Engineering. His research focuses on finding solutions for the issues related to the interactive electronic systems, integrated information systems or WSN.

Mindaugas ZILYS graduated MSc in 1996 and received his PhD in Electronics Engineering in 2001. He works as a researcher at the Department of Electronics Engineering, Faculty of Electrical and Electronics Engineering, Kaunas University of Technology and in industry. His research focuses on electronic system efficiency, energy harvesting, low power management and wireless smart sensors.